Biointerface Research in Applied Chemistry
Open-Access Journal (ISSN: 2069-5837)

Article
Volume 15, Issue 5, 2025, 70
https://doi.org/10.33263/BRIAC155.070

Synthesis and Characterization of Mixed Ligand Complexes Involving Miconazole and Salicylhydrazide with Transition Metals: Evaluation of Antibacterial and Antifungal Properties

Yasmin M.S. Jamil [1,*], Majeda M. Al-Baseer[1], Basem Al-Akhali [2]

[1] Chemistry Department, Faculty of Science, Sana'a University, Sana'a, Yemen
[2] Microbiology Department, Faculty of Science, Sana'a University, Sana'a, Yemen
* Correspondence: y.jamil@su.edu.ye;

Received: 21.03.2025; Accepted: 2.07.2025; Published: 10.08.2025

Abstract: In this study, a series of mixed-ligand transition metal complexes were synthesized using Miconazole (MCZ) and Salicylhydrazide (SH) with Cu(II), Ni(II), Zn(II), Co(II), and Cd(II) ions in ethanolic medium. The complexes were characterized by elemental analysis, FTIR, UV-Vis spectroscopy, magnetic susceptibility, molar conductivity, and powder XRD. The data support the formation of octahedral complexes, with MCZ acting as a monodentate ligand through imidazole nitrogen and SH as a bidentate ligand via C=O and NH_2 groups. Notably, the Ni(II) complex displayed 1:2 electrolyte behavior, distinct from other neutral complexes. XRD analysis confirmed nanoscale crystallinity (33–79 nm), except for the Co(II) complex, which exhibited amorphous characteristics. Antimicrobial activity was assessed against Staphylococcus aureus, Escherichia coli, Candida albicans, Penicillium italicum, and Aspergillus niger using the agar well diffusion method. The Zn(II) complex demonstrated the most significant antibacterial and antifungal activity, with inhibition zones up to 17.5 mm, surpassing both free ligands and other metal complexes. This enhancement is attributed to increased lipophilicity and reduced particle size. In contrast, Ni(II) and Co(II) complexes exhibited limited activity, particularly against Candida albicans. These findings suggest that metal coordination notably influences antimicrobial efficacy and underscore the potential of Zn(II)-based complexes for further therapeutic exploration.

Keywords: Miconazole; salicylhydrazide; transition metal complexes; antimicrobial activity; zinc complex; spectroscopic characterization; XRD.

1. Introduction

Mixed-ligand complexes have gained considerable attention in biological and medicinal chemistry due to their notable antimicrobial activities against a wide range of pathogenic microorganisms. These complexes frequently incorporate organic ligands such as phthalic, succinic, and oxalic acids, which contain donor atoms (e.g., carbonyl, nitrogen, oxygen) capable of coordinating with metal ions to yield compounds with diverse geometries and enhanced biological properties [1–3]. The biological potential of such systems has encouraged exploration into multifunctional ligands that might broaden their therapeutic utility. Among the most pharmacologically significant ligands are imidazole derivatives, such as

miconazole (Figure 1), a well-established antifungal agent listed on the World Health Organization's List of Essential Medicines. Miconazole has been used clinically since 1971 and is commonly applied topically to treat infections such as vaginal candidiasis, dermatophytosis, and other fungal skin diseases. In addition to its antifungal activity, miconazole exhibits bactericidal effects against a range of aerobic Gram-positive bacteria, though it is largely ineffective against Gram-negative species [4–6]. The inclusion of miconazole in coordination complexes is of particular interest due to its multiple coordination sites and clinically validated bioactivity.

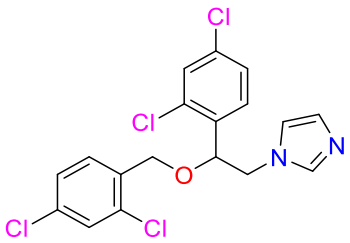

Figure 1. Chemical structure of miconazole.

On the other hand, 2-hydroxybenzoic acid hydrazide (2-HBH), as shown in Figure 2, a derivative of hydrazine where one hydrogen atom is replaced by an acyl group (RCO, R = C_6H_5OH), offers a distinct coordination environment. Hydrazides act as bidentate ligands through NH_2, C=O, and N–H donor atoms, readily forming complexes with various metal ions, particularly transition metals [7–9].

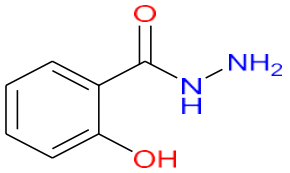

Figure 2. Chemical structure of 2-Hydroxybenzoic acid hydrazide.

There are two types of hydrazide complexes: amide (a) and imide (b) as depicted in Figure 3.

Figure 3. (a) Amide; **(b)** Imide form.

The biological relevance of hydrazides is well documented; they exhibit antibacterial [10] and tuberculostatic [11,12] properties, and their condensation products have been widely studied. However, despite the individual biological effectiveness of both miconazole and hydrazides, there remains a lack of research exploring their combined coordination behavior in mixed-ligand metal complexes. This study aims to bridge that gap by synthesizing and characterizing metal complexes incorporating both ligands.

The rationale for combining these two ligands lies in their complementary donor functionalities and biological activities. It is hypothesized that the resulting mixed-ligand complexes will display synergistically enhanced biological properties due to more effective metal ion chelation and improved molecular stability. Transition metals such as copper, nickel, zinc, cobalt, and cadmium are employed in these complexes due to their known roles in modulating antimicrobial and enzymatic functions.

Characterization of the complexes is carried out using established techniques, including UV-Vis and IR spectroscopy, as well as X-ray diffraction, to confirm structural features and evaluate potential bioactivity [13–15]. Through this work, we seek to elucidate the interplay between ligand structure and biological activity, and to contribute to the growing field of bioinorganic chemistry with novel mixed-ligand systems that exhibit promising therapeutic properties.

This study specifically investigates the synthesis, structural characterization, and biological evaluation of mixed-ligand complexes involving miconazole and 2-hydroxybenzoic acid hydrazide with selected transition metals, aiming to assess their potential as antimicrobial agents and understand the structure–activity relationships governing their performance.

2. Materials and Methods

2.1. Materials.

Miconazole (MCZ) was obtained from the International Pharmaceutical Manufacturing Company (Sana'a, Yemen). Salicylhydrazide (2-hydroxybenzoic acid hydrazide), transition metal chlorides ($MX_2 \cdot n\ H_2O$, where M = Cu(II), Ni(II), Zn(II), Co(II), Cd(II), and X = Cl^-), as well as solvents such as ethanol, dimethyl sulfoxide (DMSO), and sodium hydroxide (NaOH), were of analytical grade and purchased from commercial suppliers including BDH Chemicals Ltd. (UK) and Scharlau Chemie S.A. (Spain). All reagents were used as received without further purification.

2.2. Preparation of the complexes.

The metal complexes were synthesized by a general procedure as follows: equimolar amounts (2 mmol) of MCZ and salicylhydrazide (SH) were dissolved separately in ethanol (25 mL each), then mixed in a 100 mL round-bottom flask with continuous stirring. Subsequently, 2 mmol of the respective metal chloride salt dissolved in 20 mL of ethanol was added dropwise to the ligand mixture. The resulting reaction mixture was refluxed at $80 \pm 2°C$ for 3–4 hours using a magnetic stirrer hotplate. During reflux, a precipitate began to form, indicating complex formation. After completion, the reaction mixture was cooled to room temperature, and the solid product was filtered under vacuum. The precipitate was washed thoroughly with hot ethanol, followed by warm distilled water to remove unreacted ligands and salts. The final solid complexes were dried in a desiccator over anhydrous calcium chloride at room temperature ($25 \pm 2°C$) for 48–72 hours until constant weight was achieved. The same procedure was applied to all metal salts. All resulting complexes were solid, with distinct colors depending on the metal ion; zinc and cadmium complexes appeared colorless, while others were colored as summarized in Table 1.

2.3. Spectral measurements.

At the Yemen Standardization and Metrology Organization, the complexes were measured in the range of 400-4000 cm^{-1} by using FTIR-4800S (Shimadzu, Japan) equipment. The compounds' electronic spectra were measured at the Yemen Standardization and Metrology Organization using a UV-vis spectrophotometer (Specord40, Analytik Jena, Germany) in the 400–800 nm range. The metal content was measured by using VARIAN ICP-OES at the Yemen Standardization and Metrology Organization. Standard solutions of metal

nitrate were used for calibration. The compound's C, H, and N analyses were conducted in Vario EL Fab. CHN Nr. 11042023, at the Microicro Analytical Center, Egypt. The coordinated and uncoordinated water contents were determined gravimetrically using the weight loss method [16]. An XRD diffractometer, Rigaku (Ultima IV, USA), was utilized to gather the compounds' XRD patterns. 30 mA of current and 40 kV of voltage were employed to operate the anode made of Cu Ka (k = 1.54180 Å).

2.4. Physical measurements.

The prepared Cu (II), Ni (II), Zn (II), Cd (II), and Co (II) complexes with the mixed ligand (MCZ, SH) were collected purely after washing with hot ethanol and distilled water. All the complexes were colored, except for the Zn(II) and Cd(II) complexes,,which they were white., They were stable in air, insoluble in water and most organic solvents, but soluble in DMSO. Ni (II) and Zn (II) complexes had high melting points (> 300°C). The Cu (II), Cd (II), and Co (II) complexes had melting points of 195°C, 270°C, and 180°C, respectively.

2.5. Biological screening.

The antimicrobial activity of the synthesized ligands and their metal complexes was evaluated using the agar well diffusion method against selected standard strains: *Staphylococcus aureus* ATCC 6538 (Gram-positive), *Escherichia coli* ATCC 8379 (Gram-negative), *Aspergillus niger* ATCC 16404, *Penicillium italicum* ATCC 10129, and *Candida albicans* ATCC 10231 (fungi) [17–20].

2.5.1. Culture conditions.

Bacterial cultures were grown on Mueller–Hinton agar (MHA) and incubated at 37 °C for 24 hours, while fungal strains were cultured on Sabouraud Dextrose Agar (SDA) and incubated at 28 ± 2 °C for 48–72 hours.

2.5.2. Sample preparation and application.

The ligands and metal complexes were first dissolved in dimethyl sulfoxide (DMSO) to a stock concentration of 500 mg/L. These stock solutions were serially diluted to obtain working concentrations of 2.5, 5, 10, 50, and 100 µg/mL. Standard antimicrobial agents (e.g., Ampicillin for bacteria and fluconazole for fungi) were used as positive controls at matching concentrations for direct comparison. A microbial suspension of 1×10^8 CFU/mL was uniformly spread over the surface of the solidified agar plates. Wells of 6 mm diameter were punched using a sterile cork borer, and 100 µL of each test solution was carefully pipetted into the wells. Each test was performed in triplicate, and plates were incubated under appropriate conditions based on the microorganism type.

2.5.3. Data analysis.

After incubation, the diameters of inhibition zones (in mm) were measured using ImageJ software. The results were expressed as the mean ± standard deviation of three independent measurements.

3. Results and Discussion

3.1. Physical measurements.

The synthesized metal complexes of Cu(II), Ni(II), Zn(II), Co(II), and Cd(II) with miconazole (MCZ) and salicylhydrazide (SH) were successfully isolated as solid products following standard washing and drying procedures. All complexes appeared colored, except for those of Zn(II) and Cd(II), which were white, likely due to their d^{10} electronic configuration and diamagnetic nature. The compounds exhibited stability in air, were insoluble in water and most organic solvents, but soluble in DMSO, facilitating spectral and conductivity measurements. The melting points revealed notable thermal stability, particularly for the Ni(II) and Zn(II) complexes, which remained intact beyond 300°C, suggesting stronger metal-ligand bonding and lattice energy in these compounds. In contrast, Cu(II), Cd(II), and Co(II) complexes exhibited lower melting points (195–270°C), which may reflect differences in crystal packing or hydration levels. Molar conductance values (in DMSO, 10^{-3} M) indicated that Cu(II), Zn(II), Co(II), and Cd(II) complexes behave as non-electrolytes (Λ_m = 5.0–28.0 $S \cdot cm^2 \cdot mol^{-1}$), consistent with neutral coordination structures. However, the Ni(II) complex displayed a significantly higher conductivity (73.5 $S \cdot cm^2 \cdot mol^{-1}$), classifying it as a 1:2 electrolyte, as summarized in Table 1. This suggests the presence of two chloride ions in the outer coordination sphere, in contrast with the inner-sphere coordination observed in the other complexes.

Table 1. Some physical properties of the complexes.

Compound	Color	M.P. (°C)	PH (0.5%	Λm (Ω^{-1} cm^2 mol^{-1})
Miconazole (MCZ)	White	87	-	-
Salicylhydrazide (SH.)	White	145	-	-
[Cu (MCZ)(SH)$(H_2O)_2Cl_2$].2H_2O	Green	195	8.12	25.9
[Ni (MCZ)(SH)$(H_2O)_2$]Cl_2. H_2O	purple	>300	7.62	73.5
[Zn (MCZ)(SH)$(H_2O)_2Cl_2$]	White	>300	10.07	5.0
[Co (MCZ)(SH)$(H_2O)_2Cl_2$]	Green	180	8.89	28
[Cd (MCZ)(SH)$(H_2O)_2Cl_2$]	White	270	8.27	14.9

Elemental analysis data corroborated the proposed molecular formulas, with experimental values closely matching theoretical calculations for C, H, N, and metal contents (Table 2). These findings collectively support the successful formation of mixed-ligand complexes with distinct coordination environments depending on the metal ion involved.

Table 2. Elemental analysis of the MCZ, SH, and their metal complexes.

Compound	M.Wt (Yield%)	Element Analysis, theoretical/ (Experimental)			
		%C	%H	%N	%Metal
[Cu (MCZ)(SH)$(H_2O)_2Cl_2$] 2H_2O	756.46 (41.44)	39.66 (40.06)	3.70 (3.75)	7.40 (7.42)	8.40 (8.45)
[Ni (MCZ)(SH)$(H_2O)_2$]$Cl_2 \cdot H_2O$	769.45 (44.66)	38.99 (39.01)	3.89 (3.92)	7.28 (7.22)	7.62 (7.70)
[Zn (MCZ)(SH)$(H_2O)_2Cl_2$]	722.13 (65.63)	41.54 (41.67)	3.32 (3.32)	7.75 (7.78)	9.05 (9.09)
[Co (MCZ)(SH)$(H_2O)_2Cl_2$]	715.65 (50.00)	41.92 (41.80)	3.35 (3.40)	7.82 (7.86)	8.23 (8.26)
[Cd (MCZ)(SH)$(H_2O)_2Cl_2$]	769.16 (71.89)	39.00 (40.02)	3.12 (3.20)	7.28 (7.31)	14.61 (14.45)

3.2. Infrared spectra of miconazole and its metal complexes with salicylhydrazide.

The FTIR spectra of the free ligands (MCZ and SH) and their metal complexes provide compelling evidence for successful coordination (Table 3 and Figure 4) . Key vibrational bands observed in the free MCZ include a strong C=N stretching band at 1463 cm^{-1}, attributed to the imidazole ring. Upon complexation, this band exhibited a downward shift (~50 cm^{-1}), indicating involvement of the imidazole nitrogen in metal coordination—a well-documented behavior in imidazole-based chelates [4,5,20,21]. Salicylhydrazide exhibited characteristic O–H and N–H stretching vibrations at 3423 and 3315 cm^{-1}, respectively. These bands shifted slightly in the complexes (3272–3289 cm^{-1}), suggesting coordination through the amide NH_2 group. The amide functional group of SH showed typical bands at 1641 cm^{-1} (amide I, C=O), 1585 cm^{-1} (amide II, N–H bending), and 1243 cm^{-1} (amide III, C–N). In the complexes, these bands were shifted to higher or lower frequencies depending on the metal ion, providing further confirmation of coordination via both C=O and NH_2 groups. The phenolic C–O band remained nearly unchanged (~1027 cm^{-1}), indicating that the phenolic group is not involved in metal coordination, consistent with retention of the –OH hydrogen. Additionally [22–25], new bands in the low-frequency region (500–650 cm^{-1}) appeared in all complexes and were assigned to M–O and M–N vibrations. These bands are absent in the free ligands and confirm the formation of metal–ligand bonds through oxygen and nitrogen donor atoms [12,26].

Overall, the FTIR data support the bidentate coordination behavior of SH (via C=O and NH_2), and monodentate coordination of MCZ through the imidazole nitrogen, leading to the proposed octahedral geometry.

Table 3. FTIR of the MCZ, SH, and their metal complexes.

Assignment	MCZ	SH	[Cu(MCZ)(SH)(H_2O)$_2Cl_2$].2H_2O	[Ni(MCZ)(SH)(H_2O)$_2$Cl]Cl·H_2O	[Zn(MCZ)(SH)(H_2O)$_2Cl_2$]	[Co(MCZ)(SH)(H_2O)$_2Cl_2$]	[Cd(MCZ)(SH)(H_2O)$_2Cl_2$]
v(OH) and v(NH) and v(C-H) aromatic ring and v(C-N) imidazole	3456 3280	3458 3286	3448 3289	3449 3272	3457 3286	3423 3315	3450
v (CH_2) stretching	2932	-	2928	2926	2926	2928	2924
C=O amide I band	-	1641	1699	1695	1696	1696	1691
C-N amide II band	-	1585	1563	1563	1563	1563	1563
v(C=N)	1463	-	1412	1412	1414	1414	1413
C-N amide III band	-	1243	1273	1267	1292	1254	1280
v (C- O-C)	1089	-	1098	1093	1093	1099	1098
v (C- O)	-	1027	1024	1024	1027	1027	1030
v (C-Cl)	738	-	751	761	759	759	749
M-O M-N	-	- -	641 556	641 564	649 564	638 592	646 573

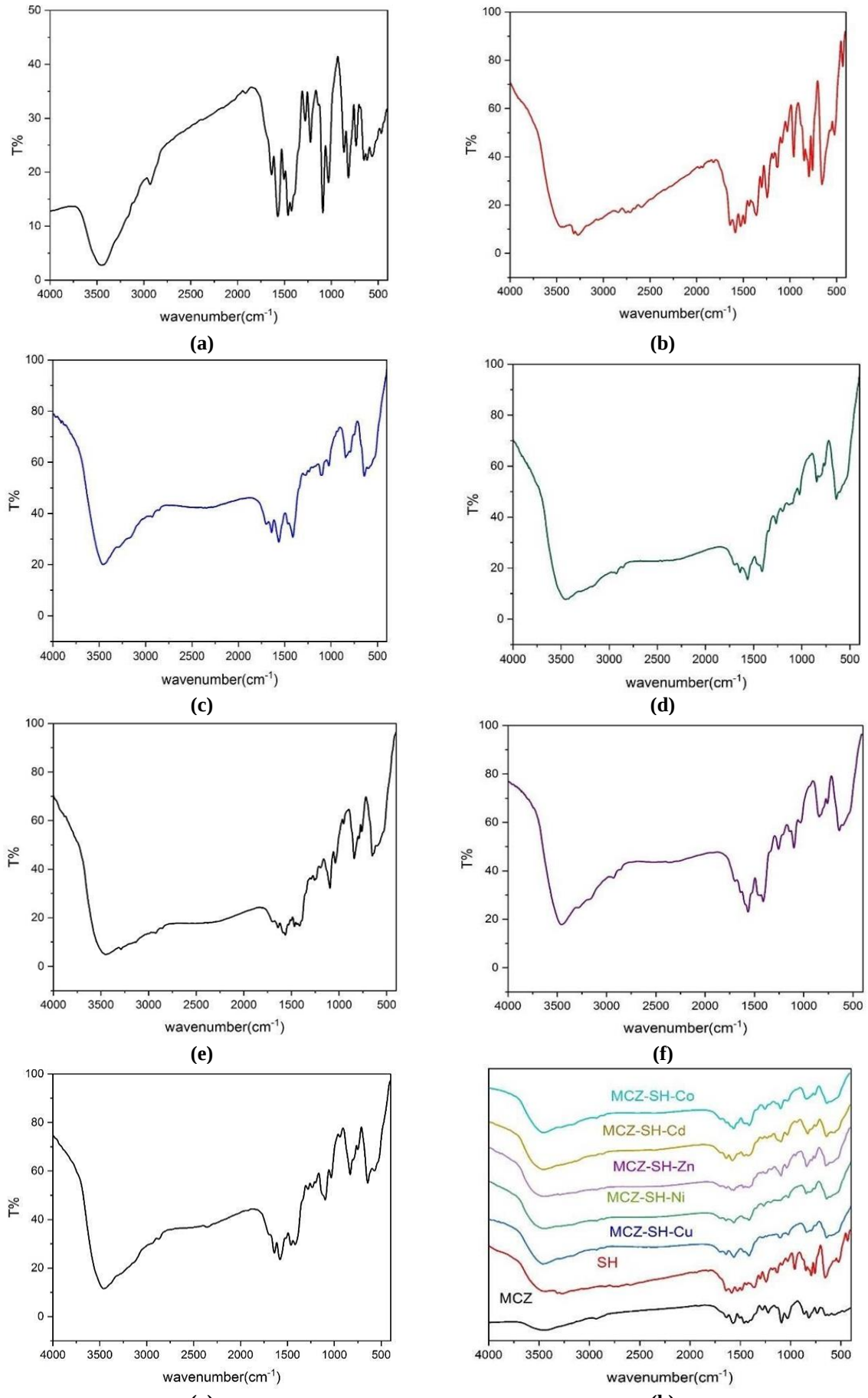

Figure 4. Infrared Spectra. **(a)** Miconazole (MCZ); **(b)** Salicylhydrazie (SH); **(c)** [Cu (MCZ)(SH)$(H_2O)_2Cl_2$] $2H_2O$; **(d)[** [Ni(MCZ)(SH)$(H_2O)_2$]$Cl_2 \cdot H_2O$; **(e)** [Zn (MCZ)(SH)$(H_2O)_2Cl_2$]; **(f)** [Co (MCZ)(SH)$(H_2O)_2Cl_2$]; **(g)** [Cd(MCZ)(SH)$(H_2O)_2Cl_2$]; **(h)** MCZ, SH ligands and their metal complexes.

3.3. Magnetic susceptibility measurements.

Magnetic susceptibility measurements provide valuable insights into the number of unpaired electrons and, consequently, the electronic structure and geometry of metal centers. The effective magnetic moment (μ_{eff}) values, calculated using Curie's law and corrected with Pascal's constants, are presented in Table 4. The Cu(II) complex exhibited a μ_{eff} of 1.74 BM, consistent with the presence of one unpaired electron in a d^9 system and suggesting an octahedral geometry with a slight tetragonal distortion, a common feature in Cu(II) complexes [26,27]. Similarly, the Ni(II) complex showed a μ_{eff} of 2.74 BM, within the expected range for a high-spin d^8 ion in an octahedral field, supporting the proposed 1:2 electrolyte structure [28]. The Co(II) complex exhibited a μ_{eff} of 3.56 BM, aligning with the expected magnetic moment for a high-spin d^7 system in an octahedral geometry. These values match well with those reported for analogous Co (II) mixed-ligand systems [29,30]. In contrast, Zn (II) and Cd (II) complexes were diamagnetic, as expected for d^{10} systems with filled orbitals, further confirming the absence of unpaired electrons and reinforcing their assigned octahedral structures [31–33].

Overall, magnetic data complement the spectral and conductivity analyses, confirming the structural integrity and electron configuration of each metal center in the synthesized complexes.

Table 4. Magnetic susceptibility of miconazole and its metal complexes with salicylhydrazide.

Compound	Color Gram susceptibility Xg x10^{-6}	Molar susceptibility XM x10^{-6}	Diamagnetic correction factor D x-10^{-6}	Atomic susceptibility XA x10^{-6}	Effective magnetic moment μeff. BM
[Cu (MCZ)(SH)(H_2O)$_2$$Cl_2$].2$H_2O$	1.65	1248	604.51	1852	1.74
[Ni (MCZ)(SH)(H_2O)$_2$] Cl_2. H_2O	4.00	3077	610.00	3692	2.74
[Co (MCZ)(SH)(H_2O)$_2$$Cl_2$]	7.25	5188	580.00	5773	3.56

3.4. Electronic spectra of miconazole and its metal complexes with salicylhydrazide.

The ultraviolet-visible spectra of various mixed ligand complexes synthesized were recorded in DMSO at room temperature and compiled in Table 5 and Figure 5.

Table 5. Magnetic moment and spectral data of the prepared compounds.

Compound	μeff (B.M.) . Cal	μeff (B.M.) .Expr	λmax (nm)	Absorption band (cm^{-1})	Assignments	Suggested structure
[Cu (MCZ)(SH)(H_2O)$_2$$Cl_2$].2$H_2O$	1.73	1.74	366-383 805	27322-26109 12422	Charge transfer L→M $^2Eg \rightarrow {}^2T_2g$	Octahedral
[Ni (MCZ)(SH)(H_2O)$_2$] Cl_2. H_2O	2.83	2.74	350 410 480	28571 24590 20833	Charge transfer L→M $^3A_2g(F) \rightarrow {}^3T_1g(P)$ $^3A_2g(F) \rightarrow {}^3T_1g(F)$	Octahedral
[Co (MCZ)(SH)(H_2O)$_2$$Cl_2$]	3.87	3.56	428 985	23364 10152	$^4T_1g(F) \rightarrow {}^4A_2g(F)$ $^4T_1g(F) \rightarrow {}^4T_2g(P)$	Octahedral
[Zn (MCZ)(SH)(H_2O)$_2$$Cl_2$]	Diamagnetic	Diamagnetic	-	-	-	Octahedral
[Cd (MCZ)(SH)(H_2O)$_2$$Cl_2$]	Diamagnetic	Diamagnetic	-	-	-	Octahedral

The electronic spectra of the free ligands and their complexes were recorded in DMSO and are summarized in Table 5 and Figure 5. Free MCZ displayed bands at 284 and 278 nm, attributable to π→π* transitions of the aromatic imidazole ring, while SH exhibited n→π* transitions at 307 and 320 nm associated with the C=O group [34].

Upon complexation, noticeable red or blue shifts occurred depending on the metal, indicating ligand-to-metal charge transfer and electronic redistribution due to coordination. For instance, the Cu(II) complex exhibited a broad d–d transition at 805 nm (12,422 cm^{-1}),

characteristic of the $^2Eg \rightarrow {}^2T_2g$ transition in an octahedral field [5,30,34], along with L→M charge transfer bands at 366–383 nm [19]. The Ni(II) complex showed three distinct absorption bands at 350 nm, 410 nm, and 480 nm, assigned to ligand-to-metal charge transfer and the transitions $^3A_2g(F) \rightarrow {}^3T_1g(F)$ and $^3A_2g(F) \rightarrow {}^3T_1g(P)$, typical for octahedral high-spin Ni(II) complexes [35,36].

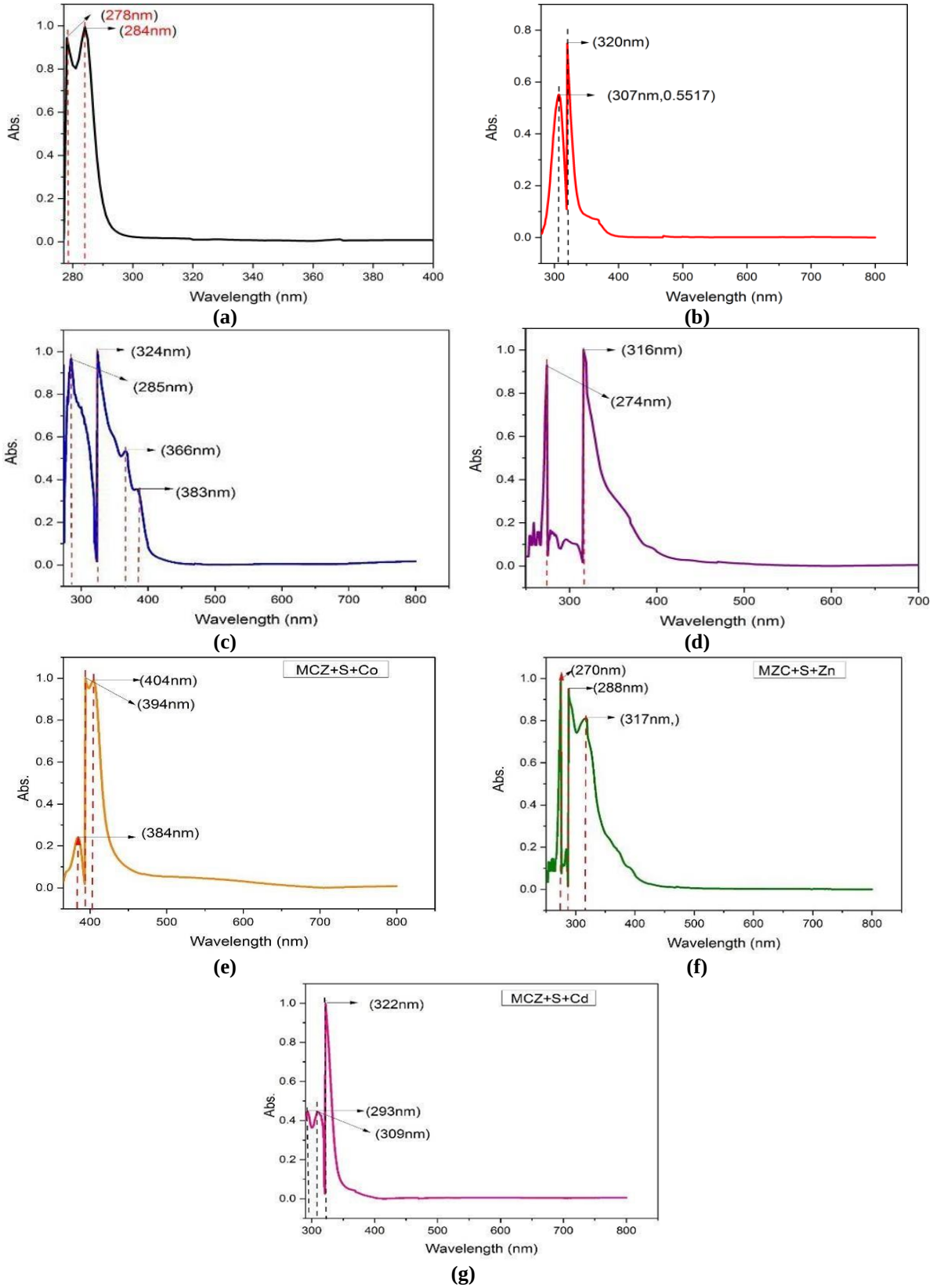

Figure 5. UV-vis spectra. **(a)** Miconazole (MCZ); **(b)** Salicylhydrazie (SH); **(c)** [Cu (MCZ)(SH)$(H_2O)_2Cl_2$].2H_2O; **(d)** [Ni(MCZ)(SH)$(H_2O)_2$]$Cl_2 \cdot H_2O$; **(e)** [Co (MCZ)(SH)$(H_2O)_2Cl_2$]; **(f)** [Zn (MCZ)(SH)$(H_2O)_2Cl_2$]; **(g)** [Cd (MCZ)(SH)$(H_2O)_2Cl_2$].

Similarly, the Co(II) complex displayed transitions at 428 nm and 985 nm, corresponding to $^4T_1g(F) \rightarrow {}^4A_2g(F)$ and $^4T_1g(F) \rightarrow {}^4T_2g(P)$, reinforcing its high-spin octahedral geometry [22,24]. No d–d transitions were observed in the Zn(II) and Cd(II) complexes due to their filled d-orbitals and diamagnetic nature, in agreement with previous studies [35–39].

These spectroscopic transitions not only support the proposed octahedral geometries (Figure 6) but also reflect the nature of metal-ligand interactions and their influence on electronic transitions.

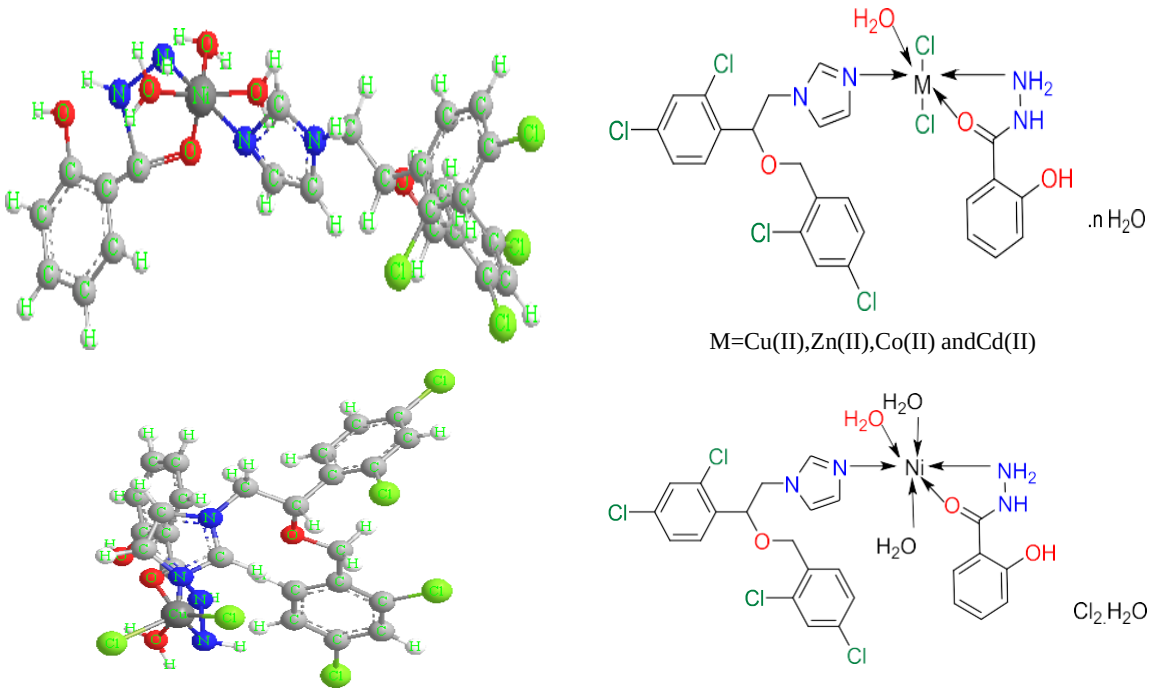

Figure 6. The proposed octahedral geometry of the prepared complexes.

3.5. X-ray diffraction.

The powder X-ray diffraction patterns of the synthesized complexes were recorded in the 2θ range of 5° to 60°, and the crystallite sizes were calculated using the Debye-Scherrer equation :$D = k\lambda / (\beta \cos\theta)$ where D is the crystallite size, k is the shape factor (0.94), λ is the Cu Kα radiation wavelength (0.15406 nm), β is the full width at half maximum (FWHM) in radians, and θ is the Bragg angle [40].

The XRD patterns(Figure 7) confirm the crystalline nature of the Cu(II), Ni(II), Zn(II), and Cd(II) complexes, with sharp and well-defined peaks indicating long-range order. The calculated average crystallite sizes ranged from 33.6 nm to 78.9 nm, placing the materials firmly in the nanocrystalline regime (Table 6). For instance, the Zn(II) complex exhibited relatively smaller crystallite size (~33.6 nm), which may contribute to its enhanced biological activity due to increased surface area and better cellular interaction, as previously reported for nanoscale antimicrobial materials [41–44].

In contrast, the Co(II) complex displayed a broad, diffused pattern without sharp peaks (Figure 7e), indicating its amorphous nature. This could be attributed to factors such as distorted coordination geometry, solvent trapping, or hydration effects during synthesis. Amorphous materials are known to exhibit distinct physicochemical behavior, including reduced biological efficacy, as observed in this case [45].

While Scherrer's equation offers a quick estimation of particle size, it does not account for microstrain, instrumental broadening, or non-uniform crystallinity, which may lead to over-

or underestimation of the true crystallite size [42]. Therefore, the values reported here should be considered approximations rather than absolute sizes.

Importantly, a tentative correlation can be observed between crystallite size and antimicrobial performance, particularly in the Zn(II) complex, whose superior activity may stem from its small size, high surface energy, and enhanced membrane permeability [44,47]. However, further studies such as TEM imaging or BET surface area analysis are recommended to confirm this relationship.

Table 6. XRD spectra data of the principal values of intensity of the (MCZ-SH-metals).

Compound	2θ	β(FWHM)	Grain Size D (nm)	Mean D
[Cu (MCZ)(SH)(H_2O)$_2$Cl2] 2H_2O	5.59	0.142	58.50177	52.69309
	14.13	0.129	64.81279	
	20.61	0.200	42.16702	
	24.44	0.152	55.85348	
	25.69	0.202	42.13039	
[Ni(MCZ)(SH)(H_2O)$_2$]Cl_2·H_2O	27.36	0.247	36.04458	42.71424
	31.70	0.194	46.35225	
	45.46	0.198	47.36792	
	56.52	0.239	41.09220	
[Zn (MCZ)(SH)(H_2O)$_2$$Cl_2$]	9.80	0.560	15.50389	33.62220
	14.60	0.388	22.47716	
	21.32	0.200	44.01179	
	22.42	0.162	54.43641	
	25.60	0.280	31.68177	
[Cd (MCZ)(SH)(H_2O)$_2$$Cl_2$]	5.08	0.160	54.11847	78.87912
	7.64	0.066	131.35924	
	15.40	0.077	113.36568	
	16.36	0.149	58.65344	
	24.72	0.240	36.89877	

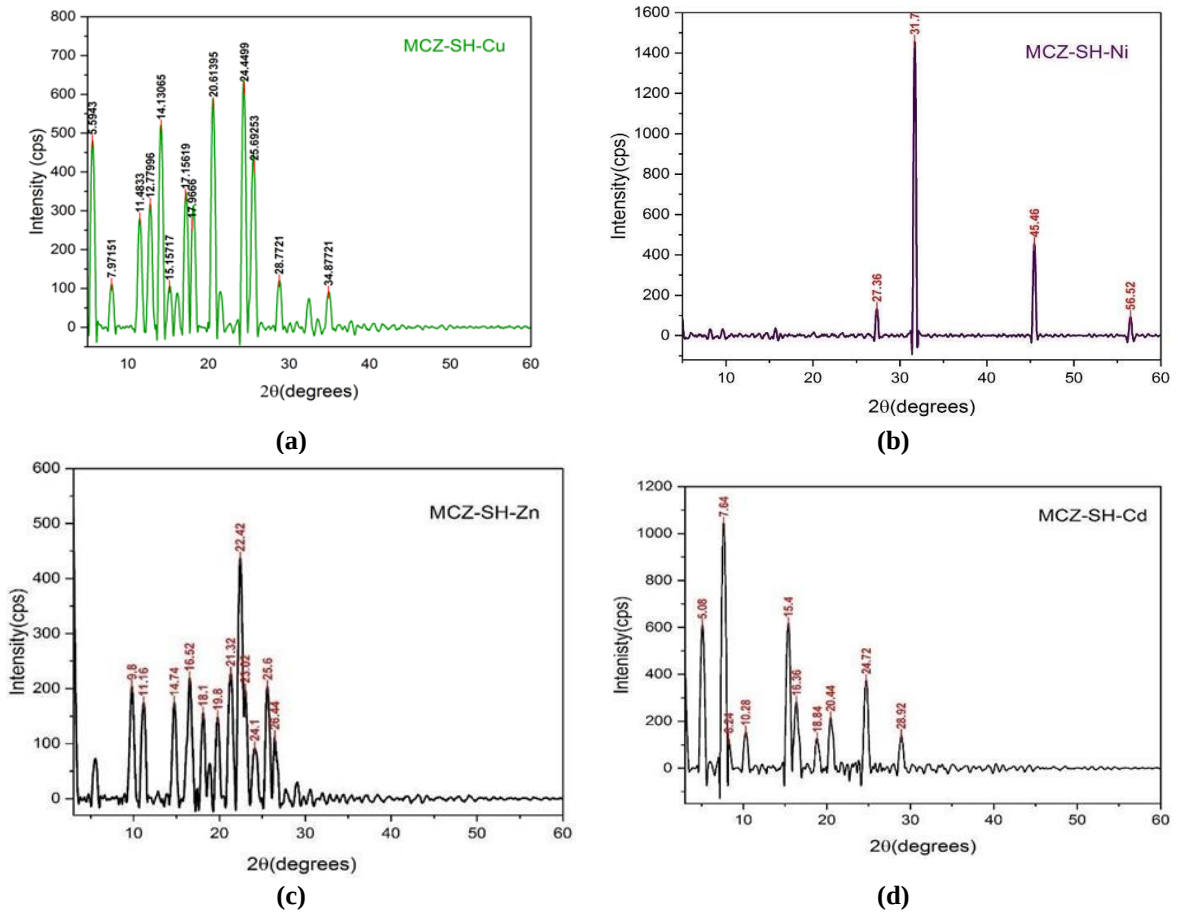

(a) **(b)** **(c)** **(d)**

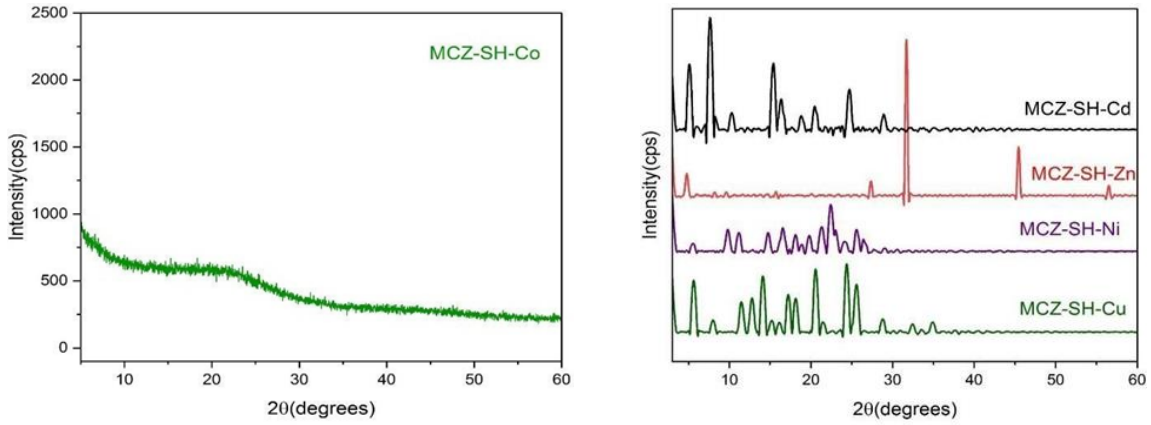

(e) **(f)**

Figure 7. XRD Spectra. **(a)** [Cu (MCZ)(SH)$(H_2O)_2Cl_2$].$2H_2O$; **(b)** [Ni(MCZ)(SH)$(H_2O)_2$]$Cl_2 \cdot H_2O$; **(c)** [Zn (MCZ)(SH)$(H_2O)_2Cl_2$]; **(d)** [Cd (MCZ)(SH)$(H_2O)_2Cl_2$]; **(e)** [Co (MCZ)(SH)$(H_2O)_2Cl_2$]; **(f)** These complexes match except Co(II) complex.

3.5.1. XRD analysis of Co (II) complex.

The XRD measurement results of the Co(II) complex are displayed in Figure 7(e). As observed in the figure, the XRD pattern exhibits a broad bump-like behavior, indicating the scattering of X-rays in all directions. This result confirms that the Co(II) complex possesses an amorphous phase [48].

3.6. Antimicrobial activity.

The antimicrobial activity of the synthesized complexes, along with the free ligands (MCZ and SH), was assessed against selected bacterial strains (*Staphylococcus aureus*, *Escherichia coli*) and fungal strains (*Candida albicans*, *Penicillium italicum*, *Aspergillus niger*) using the agar well diffusion method. Results are summarized in Table 7 and Figures 8–11.

Table 7. Antibacterial and antifungal activity of MCZ drug, SH, and their metal complexes.

Compound	mgL^{-1}	Inhibition zone diameter (mm/mg sample)				
		***S. aureus* 6538**	***E. coli* 8379**	***A. Niger.* 16404**	***P. italicum* 10129**	***C. albicans* 10231**
MCZ	2.5	0	0	6	9	7
	5	0	0	8.5	11	8
	10	0	0	9.5	13	9
	50	0	0	11	15	10
	100	0	0	14.5	17	11
Salicylhydrazide	2.5	0	0	0	4	8
	5	0	0	0	4	8
	10	0	0	0	4	8
	50	0	0	0	0	8
	100	0	0	0	0	8
[Cu (MCZ)(SH)$(H_2O)_2Cl_2$].$2H_2O$	2.5	0	0	4	8	7
	5	0	0	6.7	8	7
	10	0	0	7.5	10	8
	50	0	0	10	13	9
	100	0	0	12.5	15	9
[Ni(MCZ)(SH)$(H_2O)_2$]$Cl_2 \cdot H_2O$	2.5	0	0	0	0	7
	5	0	0	7	9.5	7
	10	0	0	8.5	10	10
	50	0	0	10	12	11
	100	0	0	12	14	11
[Zn (MCZ)(SH)$(H_2O)_2Cl_2$]	2.5	7	6	10	13.5	7.5

Compound	mgL^{-1}	Inhibition zone diameter (mm/mg sample)				
		S. aureus **6538**	***E. coli*** **8379**	***A. Niger.*** **16404**	***P. italicum*** **10129**	***C. albicans*** **10231**
	5	8	7	12	12.5	7.5
	10	9	8	15	17.5	10
	50	12	8	10	15.5	7.5
	100	14	9	17.5	17.5	10
[Co (MCZ)(SH)$(H_2O)_2Cl_2$]	2.5	0	0	5	9	7
	5	0	0	7	9	7
	10	0	0	7.5	11	8
	50	0	0	9	14	8
	100	0	0	11.5	15	11
[Cd (MCZ)(SH)$(H_2O)_2Cl_2$]	2.5	0	0	7	8	7
	5	0	0	8.5	10	7
	10	0	0	10	11	8
	50	0	0	13	13	9
	100	0	0	16.8	15	10
Standard	10	15	4.6	14	13	13

The reference standard is Ampicillin as the standard antibacterial agent, Nystatin as the standard antifungal agent.

The red value indicated the inhibition zone of the MIC.

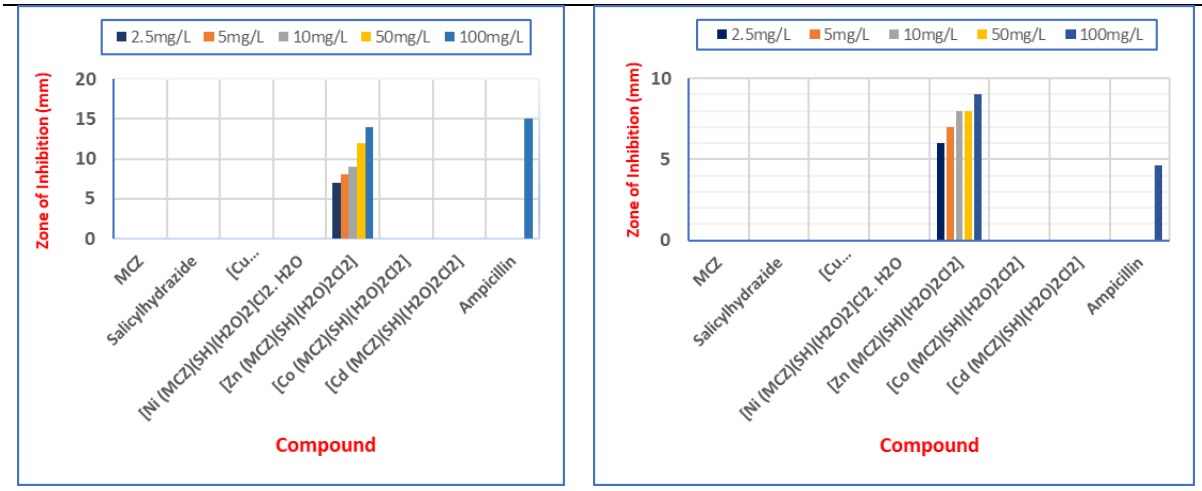

(a) **(b)**

Figure 8. Growth inhibition activity of MCZ drug, SH, and their metal complexes against bacteria: **(a)** *Staphylococcus aureus*; **(b)** *Escherichia coli.*

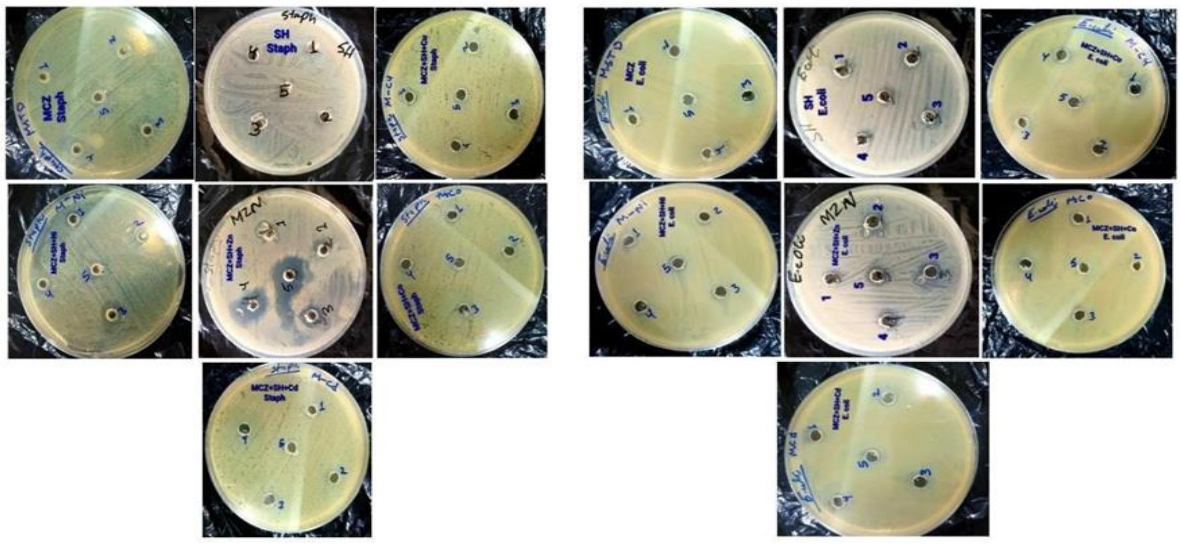

(b)

Figure 9. Antibacterial activity of MCZ drug, SH, and their metal complexes against bacteria: **(a)** *Staphylococcus aureus*; **(b)** *Escherichia coli*. Numbers refer to the concentration of ligands and complexes:2.5, 5, 10, 50, 100 mg/L.

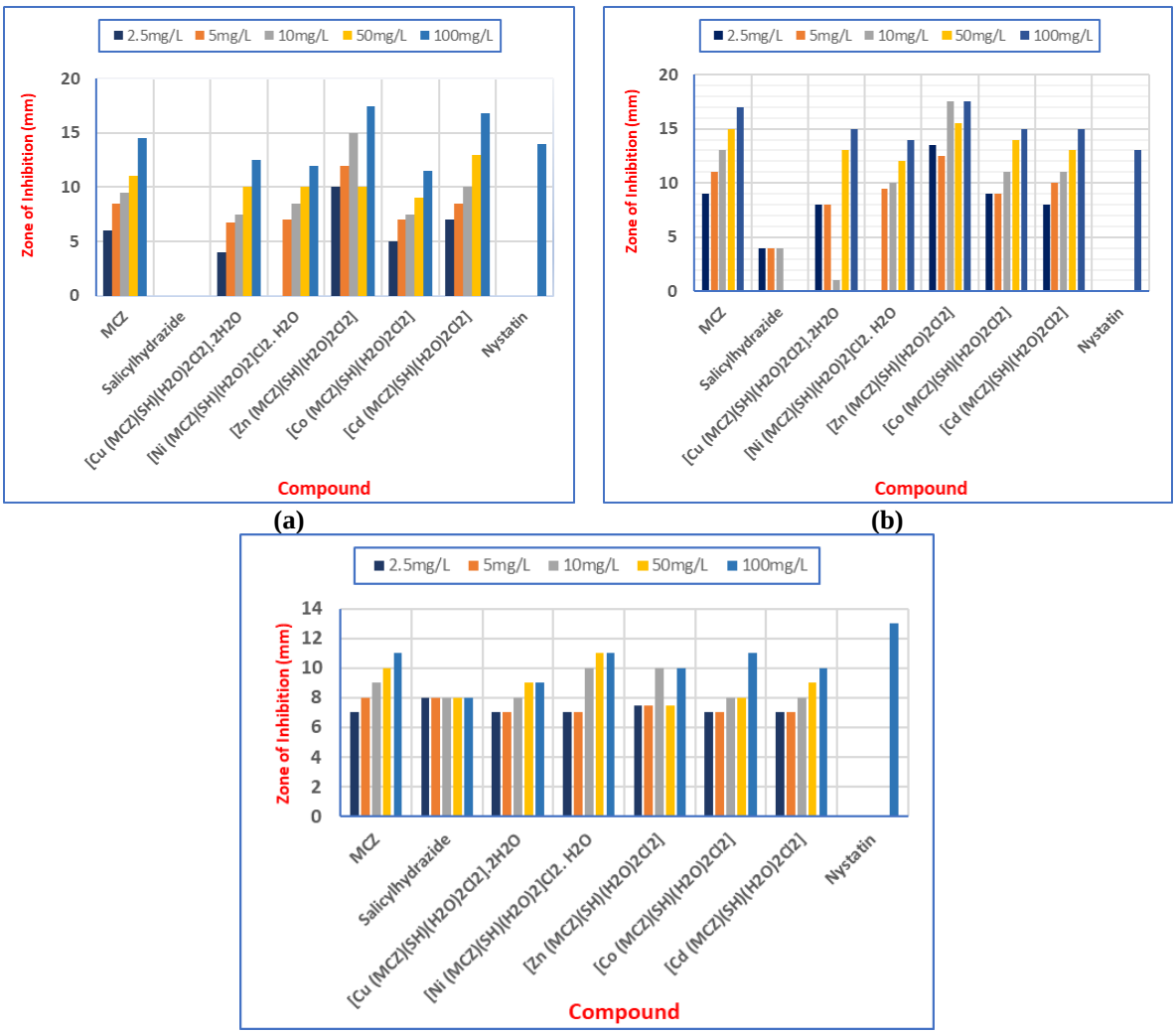

Figure 10. Growth inhibition activity of MCZ drug, SH, and their metal complexes against Fungi: **(a)** *Aspergillus Niger*; **(b)** *Penicillium italicum*; **(c)** *Candida albicans.*

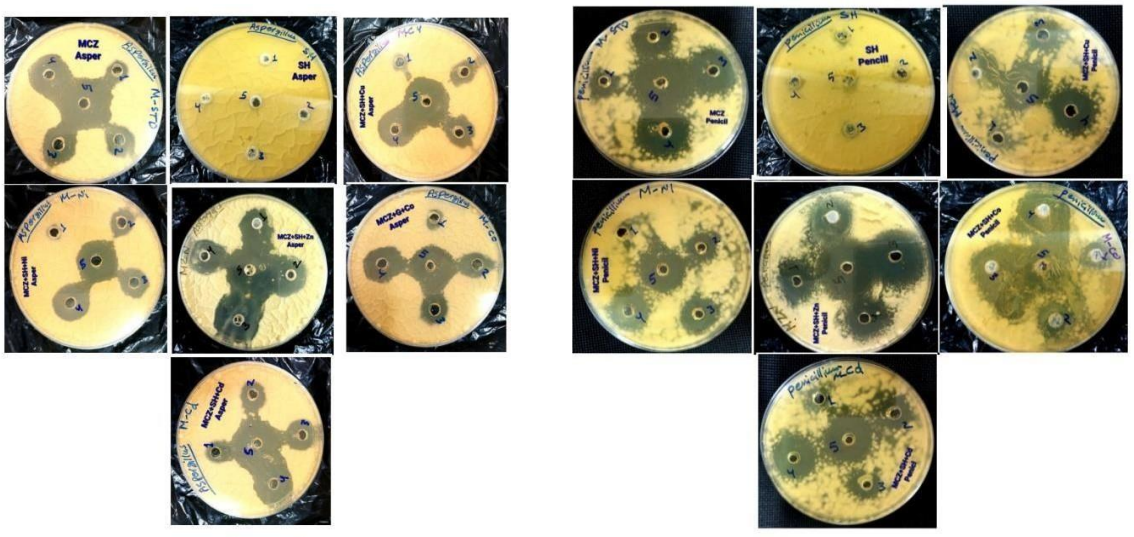

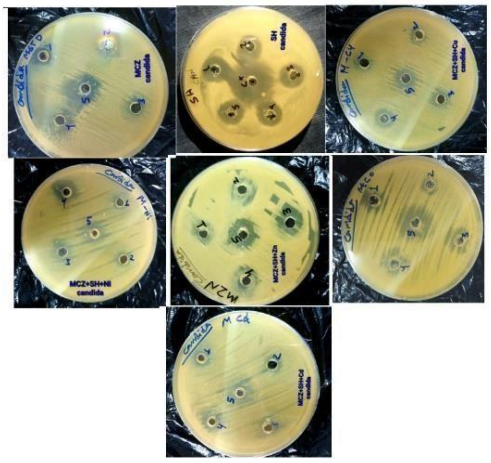

(c)

Figure 11. Antibacterial activity of MCZ drug, SH, and their metal complexes against Fungi: **(a)** *Aspergillus niger*; **(b)** *Penicillium italicum*; **(c)** *Candida albicans*.Numbers refer to the concentration of ligands and complexes: 2.5, 5, 10, 50, and 100 mg/L.

The Zn(II) complex demonstrated the most potent antibacterial and antifungal activity across all tested organisms, exhibiting inhibition zones up to 17.5 mm. This enhancement in biological activity is likely attributed to multiple physicochemical and biochemical factors. First, the relatively small crystallite size (33.6 nm) enhances the surface area-to-volume ratio, facilitating better interaction with microbial membranes. Second, the chelating effect, as described by Tweedy's theory [49], reduces the polarity of the metal ion through partial sharing of the positive charge with donor groups, increasing the complex's lipophilicity and promoting membrane penetration. Mechanistically, zinc ions have been shown to interfere with vital bacterial enzymes, such as DNA and RNA polymerases, and can disrupt membrane integrity by generating oxidative stress and interacting with thiol groups in bacterial proteins [47,48]. These effects are likely amplified when the zinc is delivered via a stable organic framework, as in the present complexes.

In contrast, the Ni(II) and Co(II) complexes exhibited limited activity, particularly against *Candida albicans*, with inhibition zones similar to those of the free MCZ ligand. This weak response could stem from several factors: larger particle size (reducing uptake), lower intrinsic antimicrobial properties of Ni and Co, or less favorable geometry for cell interaction. The Co(II) complex's amorphous structure may further hinder its biological performance due to reduced diffusion and interaction capabilities. Interestingly, all complexes exhibited superior antifungal activity compared to antibacterial effects, a trend consistent with previous studies on metal-imidazole complexes [21, 46, 49]. This may reflect the higher susceptibility of fungal membranes to disruption via metal-mediated oxidative stress.

While MIC values were not determined in this study, the concentration-dependent increase in inhibition zones (from 2.5 to 100 mg/L) confirms the dose-responsive behavior of the active complexes, particularly Zn(II). Nonetheless, future studies should include MIC and MBC/MFC assessments to enable quantitative comparison with standard antibiotics and deepen the understanding of activity thresholds.

Overall, these findings underscore the critical role of metal identity, crystallite size, coordination geometry, and lipophilicity in dictating antimicrobial efficacy. Among the tested metals, Zn(II) emerges as a promising candidate for further development due to its intrinsic antimicrobial potential and favorable coordination behavior.

3.6. Antibacterial activity analysis.

Antibacterial activity against *Escherichia coli* 8379 and *Staphylococcus aureus* 6538 was significantly absent in all tested compounds and concentrations except for the Zn(II) complex, which showed high inhibition results against both types of bacteria under study, and the results were as follows: *Staphylococcus aureus*: Effective, starting from 7 mm at 2.5 mg/L to 14 mm at 100 mg/L, and *Escherichia coli*: Shows significant activity, rising from 6 mm to 9 mm at 100 mg/L.

3.6.1. Antibacterial activity of zinc.

Zinc inhibition zones were gradually increased by the concentration increment, to reach 14 mm and 9 mm against *Staphylococcus aureus* and *Escherichia coli*, respectively, at 100 mg/L. Zinc is an essential mineral with potent antibacterial properties, disrupting bacterial functions through multiple mechanisms. It interferes with key bacterial enzymes such as carbonic anhydrase and polymerase, impairing metabolism and DNA synthesis. Zinc also interacts with the bacterial cell wall, weakening the membrane and causing essential components to leak, which results in cell death. Additionally, zinc complexes can penetrate bacterial cells and target DNA, ribosomes, and essential enzymes, enhancing their effectiveness. Zinc complexes exhibit improved physicochemical properties compared to free zinc and can be modified to increase specificity for certain bacteria. These compounds are used in developing new drugs, wound healing, and antimicrobial coatings. However, dosage control is crucial to avoid toxicity, and the potential for bacterial resistance must be monitored.

In summary, zinc and its complexes are promising tools for combating bacterial infections but require further research to optimize their efficacy and safety [48,49]. The lipophilicity of complexes is crucial for their antibacterial activity, as they deactivate cellular enzymes and impair normal cellular processes. Cell permeability, influenced by liposolubility, controls antimicrobial activity. Chelating reduces metal ion polarity and increases p-electron delocalization, enhancing complex lipophilicities. This enables simple entry into the lipid membranes of living things and the blocking of enzymes' metal binding sites [50]. Zinc's smaller particle size (33.6 nm) and lower electronegativity increase this phenomenon [51].

4. Conclusions

In this work, a series of mixed-ligand complexes of divalent transition metals with miconazole (MCZ) and salicylhydrazide (SH) were synthesized and comprehensively characterized using spectral, magnetic, and structural techniques. The data supported the formation of octahedral geometries, with MCZ coordinating via imidazole nitrogen and SH acting as a bidentate ligand through its carbonyl and amino groups. The Ni(II) complex displayed distinct electrolyte behavior, while the Co(II) complex was amorphous, in contrast to the crystalline nature of the other complexes. Biological screening revealed that complexation generally enhanced the antimicrobial activity of the ligands, particularly in the case of the Zn(II) complex, which demonstrated notable inhibition against both bacterial and fungal strains. This improvement is tentatively attributed to increased lipophilicity, nanoscale crystallinity, and zinc’s known biochemical activity. However, the activity of other complexes was less pronounced, and in some cases comparable to the free ligands. While the findings suggest a potential structure–activity relationship, the absence of detailed mechanistic studies, MIC determinations, and lipophilicity measurements limits the depth of the current molecular

mechanisms of action. Applying computational modeling or single-crystal X-ray analysis could further validate the structural assignments.

Author Contributions

Writing—original draft preparation, M.M.A.B.; investigation, M.M.A.B.; validation, Y.M.S.J.; formal analysis, Y.M.S.J., M.M.A.B., and B.A.; supervision, Y.M.S.J.; project administration, Y.M.S.J.; writing—review and editing, M.M.A.B. and Y.M.S.J. All authors have read and agreed to the published version of the manuscript.

Institutional Review Board Statement

Not applicable.

Informed Consent Statement

Not applicable.

Data Availability Statement

The data of this study will be available from the corresponding author upon reasonable request.

Funding

This research received no external funding.

Acknowledgments

This research has no acknowledgment.

Conflicts of Interest

The authors declare no conflict of interest.

References

1. Camellia, F.K.; Ashrafuzzaman, M.; Islam, M.N.; Banu, L.A.; Zahan, M.K.-E. Isoniazid Derived Schiff Base Metal Complexes: Synthesis, Characterization, Thermal Stability, Antibacterial and Antioxidant Activity Study. *Asian J. Chem. Sci.* **2022**, *11*, 23-36, https://doi.org/10.9734/ajocs/2022/v11i419131.
2. Jamil, Y.M.S.; Al-Azab, F.M.; Al-Selwi, N.A.A.; Al-Ryami, A.M.; Mlahia, M.R. Spectroscopic and biological studies of mixed ligand complexes of transition metal (II) ions with chloroquine and ketoprofen. *Sana'a Univ. J. Appl. Sci. Technol.* **2024**, *2*, 53-64, https://doi.org/10.59628/jast.v2i1.801.
3. Khalaf, M.M.; Abd El-Lateef, H.M.; Gouda, M.; Abdelhamid, A.A.; Amer, A.A.; Alfarsi, A.; Almarri, M.N.; Abdou, A. New phthalazine based nickel (II), cobalt (II), and copper (II) mixed-ligand complexes; characterization, physicochemical properties, anti-inflammatory, antifungal, antibacterial, DFT and molecular docking exploration. *J. Indian Chem. Soc.* **2024**, *101*, 101191, https://doi.org/10.1016/j.jics.2024.101191.
4. Stryjska, K.; Korona-Glowniak, I.; Chęcińska, L.; Kusz, J.; Ochocki, J. Synthesis, Spectroscopy, Single-Crystal Structure Analysis and Antibacterial Activity of Two Novel Complexes of Silver(I) with Miconazole Drug. *Int. J. Mol. Sci.* **2021**, *22*, 1510, https://doi.org/10.3390/ijms22041510.
5. Alshehri, N.S.; Sharfalddin, A.A.; Domyati, D.; Basaleh, A.S.; Hussien, M.A. Experiment versus theory of copper (II) complexes based imidazole derivatives as anti-cancer agents. *J. Indian Chem. Soc.* **2022**, *99*, 100692, https://doi.org/10.1016/j.jics.2022.100692.

6. Kelemen, H.; Hancu, G.; Gâz-Florea, S.A.; Nemes-Nagy, E.; Papp, L.A.; Mircia, E. Characterization of Inclusion Complexes between Miconazole and Different Cyclodextrin Derivatives. *Acta Marisiensis - Seria Med.* **2018**, *64*, 70-76, https://doi.org/10.2478/amma-2018-0012.
7. Mohamed, M.H.; Nadher, A.A.; Mohamed, A.I.; Ehab, A.-L. Synthesis of 1,2-dihydropyridine, Arylidene, Hydrazide, and Terthienylnicotinamidine Hydrochloride Analogs: Theoretical Studies, and Antioxidant Activity Assessment. *Curr. Org. Chem.* **2023**, *27*, 546-556, https://doi.org/10.2174/1385272827666230614123355.
8. Majumdar, P.; Pati, A.; Patra, M.; Behera, R.K.; Behera, A.K. Acid Hydrazides, Potent Reagents for Synthesis of Oxygen-, Nitrogen-, and/or Sulfur-Containing Heterocyclic Rings. *Chem. Rev.* **2014**, *114*, 2942-2977, https://doi.org/10.1021/cr300122t.
9. Jamil, Y.; Al-Baseer, M.M.; Al-Akhali, B.; Alhakimi, A.N. Synthesis and characterization of mixed ligand complexes of Fluconazole drug and glycine with some transition metals: antifungal study. *Sana'a Univ. J. Appl. Sci. Technol.* **2025**, *3*, 718-729, https://doi.org/10.59628/jast.v3i2.1534.
10. Pavan, F. R.; da S Maia, P. I.; Leite, S. R.; Deflon, V. M.; Batista, A. A.; Sato, D. N.; Franzblau, S. G.; Leite, C. Q. Thiosemicarbazones, semicarbazones, dithiocarbazates and hydrazide/hydrazones: anti-Mycobacterium tuberculosis activity and cytotoxicity. *European Journal of Medicinal Chemistry*, **2010**, *45*(5), 1898–1905. https://doi.org/10.1016/j.ejmech.2010.01.028
11. Marastoni, M.; Baldisserotto, A.; Trapella, C.; McDonald, J.; Bortolotti, F.; Tomatis, R. HIV protease inhibitors: synthesis and activity of *N*-aryl-*N′*-hydroxyalkyl hydrazide pseudopeptides. *Eur. J. Med. Chem.* **2005**, *40*, 445-451, https://doi.org/10.1016/j.ejmech.2004.11.016.
12. Bajracharya, P.; Shrestha, S. Coordination Behaviour Of 2-Hydroxybenzoic Acid Hydrazide Towards Nickel (II) And Cobalt(II): Spectroscopic Investigation. *Sci. World* **2021**, *14*, 37-43, https://doi.org/10.3126/sw.v14i14.34981.
13. Nakamoto, K. Infrared and Raman Spectra of Inorganic and Coordination Compounds, Part B: Applications in Coordination, Organometallic, and Bioinorganic Chemistry, 6th Edition; John Wiley & Sons, Inc: **2009**; https://doi.org/10.1002/9780470405888.
14. Silverstein, R.M.; Bassler, G.C. Spectrometric identification of organic compounds. *J. Chem. Educ.* **1962**, *39*, 546, https://doi.org/10.1021/ed039p546.
15. Lever, A.B.P. Inorganic Electronic Spectroscopy. Elsevier: Amsterdam, The Netherlands, **1968**.
16. Vogel, A.I. A Textbook of Quantitative Inorganic Analysis, 5th ed.; Longmans: London, UK, **1989.** chem.hbcse.tifr.res.in/wp-content/uploads/2019/10/vogels-textbook-of-quantitative-chemical-analysis-5th-edition.pdf
17. Al-Azab, F.M.; Jamil, Y.M.S.; Al-Gaadbi, A.A.M. Synthesis and Spectroscopic methods on the complexation of Co^{II}, Ni^{II} and Cu^{II} with 2-(((1H-indol-3-yl) methylene) amino) acetohydrazide hydrate. *Sana'a Univ. J. Appl. Sci. Technol.* **2023**, *1*, 103-119, https://doi.org/10.59628/jast.v1i1.131.
18. Kasim, S. M.; Al-Bazzaz, F. Y.; Hammoodi, S. H.; Mustafa, Y. F. A review of Schiff base-inorganic complexes and recent advances in their biomedicinal and catalytic attributes. *Poly. Arom. Com*, **2023**, *5*, 522-535. https://doi.org/10.22034/ecc.2023.379484.1587.
19. Al-Adilee, K.J. Synthesis, Spectral, Thermal and Biological Studies of Some Metal Complexes Derived From Heterocyclic Mono-Azo Dye Ligand 2′[2′-Hydroxy-4-methylphenyl) azo] imidazole. *Asian J. Chem* **2018**, *30*, 280-292.
20. Abd El-Halim, H.F.; Nour El-Dien, F.A.; Mohamed, G.G.; Mohamed, N.A. Synthesis, spectroscopic, thermal characterization, and antimicrobial activity of miconazole drug and its metal complexes. *J. Therm. Anal. Calorim.* **2012**, *109*, 883-892, https://doi.org/10.1007/s10973-011-1784-2.
21. Simpson, P.V.; Nagel, C.; Bruhn, H.; Schatzschneider, U. Antibacterial and Antiparasitic Activity of Manganese(I) Tricarbonyl Complexes with Ketoconazole, Miconazole, and Clotrimazole Ligands. *Organometallics* **2015**, *34*, 3809-3815, https://doi.org/10.1021/acs.organomet.5b00458.
22. Salami, H.A.; Haruna, A.U.; Ezeala, F.T.; Salawu, O.W. Solvent-free synthesis, characterization and antimicrobial activity of complexes of 2-hydroxybenzoic acid hydrazide with some M(II) chlorides (M= Co and Ni). *Der Pharma Chem*. **2015**, *7*, 261-265.
23. Júnior, Z.S.S.; Botta, S.B.; Ana, P.A.; França, C.M.; Fernandes, K.P.S.; Mesquita-Ferrari, R.A.; Deana, A.; Bussadori, S.K. Effect of papain-based gel on type I collagen - spectroscopy applied for microstructural analysis. *Sci. Rep.* **2015**, *5*, 11448, https://doi.org/10.1038/srep11448.
24. Mach, J. Complex compounds of cobalt(II) salts with salicylhydrazide. *Chem. Pap.* **1975**, *29*, 582-589.

25. Issa, R.M.; El-Shazly, M.F.; Iskander, M.F. Coordination compounds of hydrazine derivatives with transition metals. I. Metal chelates with benzhydrazide and salicylhydrazide. *Z. Anorg. Allg. Chem*. **1967**, *354*, 90-97. https://doi.org/10.1002/zaac.19673540118.
26. Al-Azab, F.M.; Jamil, Y.M.; Al-Gaadbi, A.A. Synthesis, structural and spectroscopic properties of Co(II), Ni(II) and Cu(II) complexes with 2-((2-chlorobenzylidene)amino) acetohydrazide hydrate and their Antimicrobial and antioxidant activities. *Eclética Química* **2023**, *48*, 66-82, https://doi.org/10.26850/1678-4618eqj.v48.2.2023.p66-82.
27. Ramírez-Contreras, D.; García-García, A.; Mendoza, A.; Serrano-de la Rosa, L. E.; Sánchez-Gaytán, B. L.; Melendez, F. J.; Castro, M. E.; González-Vergara, E. D,L-Citrullinato-bipyridine Copper Complex: Experimental and Theoretical Characterization. *Crystals*, **2023**, *13*(9), 1391. https://doi.org/10.3390/cryst13091391
28. Hasty, E.F. Magnetic Exchange Interactions in Dimeric and Polymeric Transition-Metal Complexes. Doctoral Thesis, University of Illinois, Urbana, IL, USA, **1974**.
29. Housecroft, C.E.; Sharpe, A.G. Inorganic Chemistry, 3rd Edition; Pearson Education Limited: **2008**.
30. Gopalan, R. Concise Coordination Chemistry; Vikas Publication House Pvt Ltd: **2001**.
31. Abdalrazaq, S.M.; Suleiman Hamad, I.; Saber Shihab, A. Synthesis, Characterization, and Biological Activity of 5-Chloroquinolin-8-ol Complexes. *Macromol. Symp.* **2025**, *414*, 2400224, https://doi.org/10.1002/masy.202400224.
32. El-Tabl, A.S.; El-Wahed, M.M.A.; El Kadi, N.M.; Kolkaila, S.A.; Samy, M. Novel Metal Complexes of Bioactive Amide Ligands as New Potential Antibreast Cancer Agents. *TWIST* **2023**, *18*, 151-169.
33. Benner, F.; La Droitte, L.; Cador, O.; Le Guennic, B.; Demir, S. Magnetic hysteresis and large coercivity in bisbenzimidazole radical-bridged dilanthanide complexes. *Chem. Sci.* **2023**, *14*, 5577-5592, https://doi.org/10.1039/D3SC01562A.
34. Alibrahim, K.A.; Alsuhaibani, A.M.; Refat, M.S. Synthesis and spectroscopic characterizations of manganese(II), iron(III), copper(II) and zinc(II) hydrazine complexes as catalytic activity agents. *Bull. Chem. Soc. Ethiop*. **2022**, *36*, 33-44, https://doi.org/10.4314/bcse.v36i1.4.
35. Abd-Elzaher, M.M. Spectroscopic Characterization of Some Tetradentate Schiff Bases and Their Complexes with Nickel, Copper and Zinc. *J. Chin. Chem. Soc.* **2001**, *48*, 153-158, https://doi.org/10.1002/jccs.200100027.
36. Mohamed, G.G.; El-Gamel, N.E.A. Synthesis, investigation and spectroscopic characterization of piroxicam ternary complexes of Fe(II), Fe(III), Co(II), Ni(II), Cu(II) and Zn(II) with glycine and $_{DL}$-phenylalanine. *Spectrochim. Acta A Mol. Biomol. Spectrosc.* **2004**, *60*, 3141-3154, https://doi.org/10.1016/j.saa.2004.01.035.
37. Karem, L.K.A. Synthesis, Characterization and Biological Evaluation of New Schiff Bases Mixed Ligand Metal Complexes of Some Drug Substances. Dissertation Thesis, University of Baghdad, Baghdad, Iraq, **2016**.
38. Aly, S.A.; Hassan, S.S.; El-Boraey, H.A.; Eldourghamy, A.; Abdalla, E.M.; Alminderej, F.M.; Elganzory, H.H. Synthesis, Biological Activity, and the Effect of Ionization Radiation on the Spectral, XRD, and TGA Analysis of Cu(I), Cu(II), Zn(II), and Cd(II) Complexes. *Arab. J. Sci. Eng.* **2024**, *49*, 361-379, https://doi.org/10.1007/s13369-023-07988-2.
39. Ahmed, R.M.; Rahman, S.S.A.; Badri, D.H.; Sultan, K.M.; Majeed, I.Y.; Kamil, G.M. Synthesis, Characterisation and Biological Activity of New Co, Ni, Zn and Cd Polymeric Complexes Derived from Dithiocarbamate Ligand. *Baghdad Sci. J.* **2024**, *21*, 384-400, https://doi.org/10.21123/bsj.2023.8038.
40. Jamil, Y.M.S.; Al-Azab, F.M.; Al-Selwi, N.A.; Alorini, T.; Al-Hakimi, A.N. Preparation, physicochemical characterization, molecular docking and biological activity of a novel schiff-base and organophosphorus schiff base with some transition metal(II) ions. *Main Group Chem.* **2023**, *22*, 337-362, https://doi.org/10.3233/MGC-220101.
41. Jaiswal, J.; Gandhi, S. A.; Padariya, T. J.; Barot, V.; Patel, U. H. Synthesis and x-ray powder diffraction studies: metal complexes (co (ii), ni (ii) and cu (ii)) of schiff base ligand 4-bromo-2-chloro-6-[(1z)-n-(phenyl) ethanimidoyl] phenol. *Journal of Pure and Applied Sciences* **2017**, *24 – 25*, 101 – 105.
42. Awate, R.; Mishra, A.; Mansuri, A. Synthesis and Characterization of Transition Metal complexes with pyrimidine based ligand derivative. *J. Phys. Conf. Ser.* **2016**, *755*, 012019, https://doi.org/10.1088/1742-6596/755/1/012019.
43. Cao, G. Nanostructures and Nanomaterials: Synthesis, Properties and Applications. Imperial College Press: **2004**.

44. Hakimi, M.; Moeini, K.; Mardani, Z.; Khorrami, F. Crystal Structure and Characterization of a New Eight Coordinated Cadmium Complex. *J. Korean Chem. Soc.* **2013**, *57*, 352-356, https://doi.org/10.5012/jkcs.2013.57.3.352.
45. Buldurun, K.; Turan, N.; Savci, A.; Alan, Y.; Colak, N. Synthesis, Characterization, X-Ray Diffraction Analysis of A Tridentate Schiff Base Ligand and Its Complexes with Co(II), Fe(II), Pd(II) and Ru(II): Bioactivity Studies. *Iran. J. Chem. Chem. Eng.* **2022**, *41*, 2635-2649, https://doi.org/10.30492/ijcce.2021.531629.4775.
46. Jamil, Y.M.; Al-Azab, F.M.; Al-Selwi, N.A. Novel organophosphorus Schiff base ligands: Synthesis, characterization, ligational aspects, XRD and biological activity studies. *Eclética Química* **2023**, *48*, 36-53, https://doi.org/10.26850/1678-4618eqj.v48.3.2023.p36-53.
47. Qadir, G.; Hadi, H. Electrodeposition of Nickel-copper alloy from aqueous solutions in the presence oforganicadditives. *Zanco Journal of Pure and Applied Sciences*, **2023**, *35*(3), 197–207. https://doi.org/10.21271/ZJPAS.35.3.18.
48. Abendrot, M.; Chęcińska, L.; Kusz, J.; Lisowska, K.; Zawadzka, K.; Felczak, A.; Kalinowska-Lis, U. Zinc(II) Complexes with Amino Acids for Potential Use in Dermatology: Synthesis, Crystal Structures, and Antibacterial Activity. *Molecules* **2020**, *25*, 951, https://doi.org/10.3390/molecules25040951.
49. Ishida, S.T. Anti-Bacterial Vaccine Activities of Bacteriolyses by Zn^{2+} -Induced Peptidoglycan Autolysins and Zinc-, ZnONPsDependent Lyses in Bacterial Cell Walls. *Int. J. Res. Stud. Med. Health Sci.* **2019**, *4*, 2-13.
50. Patil, A.; Chakraborty, S.; Yadav, Y.; Sharma, B.; Singh, S.; Arya, M. Bioremediation strategies and mechanisms of bacteria for resistance against heavy metals: a review. *Bioremediat. J.* **2024**, 1-33, https://doi.org/10.1080/10889868.2024.2375204.
51. Refat, M.S.; Al-Maydama, H.M.A.; Al-Azab, F.M.; Amin, R.R.; Jamil, Y.M.S. Synthesis, thermal and spectroscopic behaviors of metal–drug complexes: La(III), Ce(III), Sm(III) and Y(III) amoxicillin trihydrate antibiotic drug complexes. *Spectrochim. Acta A Mol. Biomol. Spectrosc.* **2014**, *128*, 427-446, https://doi.org/10.1016/j.saa.2014.02.160.

Publisher's Note & Disclaimer